

Effect of Varying Ladle Stream Temperature on the Melt Flow and Heat Transfer in Continuous Casting Tundishes

Sanjib CHAKRABORTY and Yogeshwar SAHAI¹⁾

Graduate Student, The Ohio State University, 116 West 19th Avenue, Columbus, OH 43210, U.S.A. 1) Department of Materials Science and Engineering, The Ohio State University, 116 West 19th Avenue, Columbus, OH 43210, U.S.A.

(Received on February 28, 1991; accepted in final form on April 26, 1991)

The effect of varying ladle stream temperature on the fluid flow and heat transfer phenomena in a typical twin strand slab caster tundish has been mathematically modeled in the present study. The model involves solution of the transient, three dimensional form of the turbulent Navier–Stokes' equation, along with the equations of turbulence energy, energy dissipation rate of turbulence energy and thermal energy conservation. The incoming melt stream temperature has been assumed to decline at a constant rate of 0.5°C/min over a casting period of 50 min. Under the conditions examined in the present mathematical model, the temperature of the incoming melt stream becomes lower than the bulk temperature of the melt in the tundish by about 1–2°C, after 25 min from the start of teeming of a heat. Due to buoyancy effects, the cooler incoming melt starts to flow along the bottom of the tundish instead of the normal top free surface directed flow. The calculations show that the inverse flow pattern develops over the remainder of the teeming period and persists for about 1 min into the teeming of the next heat. Thus, the inclusion flotation and removal of the non-metallic inclusions during the later half of the casting period are expected to be worse compared to the first half.

KEY WORDS: tundish; ladle melt stream; temperature inversion; reverse melt flow; mathematical modeling.

1. Introduction

To date, mathematical modeling studies of fluid flow and heat transfer in continuous caster tundishes have been done assuming steady state conditions, *i.e.* no variation of the flow or thermal state of the fluid with time.^{1–3)} However, fluid flow and heat transfer phenomena in actual tundishes are rarely invariant with time. The most obvious example of transient phenomena in a tundish occurs during the ladle change operation. The consequent transient fluid flow and thermal fields existing in the tundish have been mathematically modeled, and their effect on the flotation and removal of non-metallic inclusions in the melt have been discussed by the authors in their previous paper.⁴⁾

Apart from the ladle change operation, unsteady state situation can be seen to exist within the tundish for the whole extent of the casting period if the variation of the ladle stream temperature with time is considered. In an actual industrial operation, the temperature of the melt teemed from the ladle to the tundish decreases continuously with time. This is due to the continuous heat loss of the melt contained in the ladle, by radiation from the top surface and by conduction and convection from the side walls and bottom. Typical casting periods are usually 50 min or more for each ladle. Thus, the temperature of the melt during the later stages of teeming is lower compared to the temperature of the melt cast

initially. The effect of this temperature differential of the ladle melt stream on the fluid flow and heat transfer phenomena of the melt in the tundish has been investigated in the present paper.

2. Model Formulation

The system chosen for the present investigation is a two-strand slab caster tundish with weirs and dams as the flow modification devices. The design parameters of the tundish and the thermophysical parameters and properties of molten steel and refractory used are given in **Table 1**. Due to symmetry considerations, only a quarter of the full tundish has been modeled (**Fig. 1**). For modeling the effect of the varying temperature of the incoming melt on the flow and heat transfer phenomena in the tundish, two consecutive casting periods of 50 min each were considered. The temperature of the ladle outlet stream was assumed to decline at a constant rate of 0.5°C/min over the full 50 min of the teeming period. This rate of temperature drop is commonly observed in actual practice and has been cited often in the literature.^{5–7)} The melt depth was assumed to remain at the normal operating level of 1.15 m throughout the casting period. The effect of the ladle change occurring between two successive heats on the fluid flow and heat transfer phenomena in the tundish has already been presented by the authors in a previous

Table 1. Important parameters for modeling of fluid flow and heat transfer in the tundish.

Length of tundish	8.0 m
Width of tundish	1.0 m
Depth of melt	1.15 m
Inlet diameter	0.10 m
Outlet diameter	0.10 m
Number of strands	2
Distance of weir from the inlet	0.45 m
Depth of weir in the melt	0.70 m
Distance of dam from the inlet	0.90 m
Height of dam	0.60 m
Inlet velocity	1.52 m sec ⁻¹
Density of steel	$\rho = 7010 + (T - T_{m,p})(-0.883) \text{ kg m}^{-3}$ *
Specific heat capacity of steel	750 J kg ⁻¹ K ⁻¹
Thermal conductivity of steel	41.0 W m ⁻¹ K ⁻¹
Thickness of refractory	0.20 m
Thermal conductivity of refractory	1.5 W m ⁻¹ K ⁻¹

* $T_{m,p}$ = Melting point of iron.

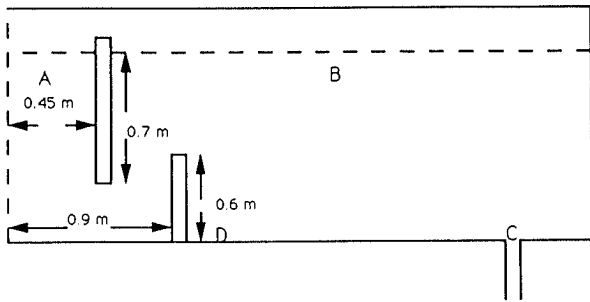


Fig. 1. Schematic of a quarter of the tundish with a dam and a weir, and the location of the four temperature monitoring points.

paper.⁴⁾ Thus, in the present investigation, the melt depth was assumed to be at the steady state level throughout the duration of the two heats.

The governing equations representing the mathematical model are:

Equation of Continuity –

$$\frac{\partial \rho}{\partial t} + \frac{\partial(\rho u_i)}{\partial x_i} = 0 \dots\dots\dots(1)$$

Momentum Balance Equations –

$$\frac{\partial(\rho u_i)}{\partial t} + \frac{\partial(\rho u_i u_j)}{\partial x_j} - \frac{\partial p}{\partial x_i} + \frac{\partial}{\partial x_j} \left[\mu_{\text{eff}} \left\{ \frac{\partial u_i}{\partial x_j} + \frac{\partial u_j}{\partial x_i} \right\} \right] + g_i(\rho - \rho_0) \dots\dots\dots(2)$$

Turbulent Kinetic Energy –

$$\frac{\partial(\rho k)}{\partial t} + \frac{\partial}{\partial x_i} \left[\rho u_i k - \frac{\mu_{\text{eff}}}{\sigma_k} \frac{\partial k}{\partial x_i} \right] = G - \rho \varepsilon \dots\dots\dots(3)$$

Dissipation Rate of Turbulence Energy –

$$\frac{\partial(\rho \varepsilon)}{\partial t} + \frac{\partial}{\partial x_i} \left[\rho u_i \varepsilon - \frac{\mu_{\text{eff}}}{\sigma_\varepsilon} \frac{\partial \varepsilon}{\partial x_i} \right] = (C_1 \varepsilon G - C_2 \rho \varepsilon^2) / k \dots\dots\dots(4)$$

where

$$G = \mu_t \frac{\partial u_i}{\partial x_i} \left[\frac{\partial u_i}{\partial x_j} + \frac{\partial u_j}{\partial x_i} \right] \dots\dots\dots(5)$$

$$\text{Effective viscosity, } \mu_{\text{eff}} = \mu_t + \mu_t \dots\dots\dots(6)$$

$$\mu_t = C_D \rho k^2 / \varepsilon \dots\dots\dots(7)$$

Thermal Energy Conservation –

$$\frac{\partial(\rho T)}{\partial t} + \frac{\partial(\rho u_i T)}{\partial x_i} = \frac{\partial}{\partial x_i} \left[\rho k_{\text{eff}} \frac{\partial T}{\partial x_i} \right] \dots\dots\dots(8)$$

The values of the various constants in the turbulence model follow the recommendations of Launder and Spalding.⁸⁾

3. Boundary Conditions

Close to the tundish walls, the variation in the flow properties are much steeper than within the bulk fluid. The velocities parallel to the walls and the turbulence quantities at the nearwall nodes were calculated using the standard logarithmic wall functions.⁹⁾ At the free surface which was assumed to be flat and at the symmetry planes, the normal velocity components and the normal gradients of the parallel velocity components, turbulence energy and energy dissipation were set to be zero. For modeling the heat losses in the tundish, a heat flux of 15 kW/m² was specified at the free surface.¹⁰⁾ A temperature wall function following Jayatilake's correlation¹¹⁾ was used to calculate heat losses through the walls. The heat loss through the thermal boundary layer as given by the correlation¹¹⁾ was equated to the conduction heat loss through the walls and natural convection heat transfer at the outside surfaces of the walls. Appropriate heat transfer correlations were taken from Ref. 12). An ambient air temperature of 323 K was assumed. The computed steady state heat losses were 1.4 kW/m² from the bottom, 3.2 kW/m² from the longitudinal, vertical wall and 3.8 kW/m² from the transverse, vertical wall. These values are in good agreement with the industrially measured conduction heat loss value of 2.6 kW/m², quoted in Ref. 3). At the symmetry planes, the normal gradients of temperature were taken to be zero.

As mentioned before, the total casting time of a heat considered in the present modeling study was 50 min. Assuming a constant teeming rate from a 250 t ladle, the tundish inlet velocity was calculated to be 1.52 m/sec. In an actual system, the velocity of the melt stream coming out of the ladle decreases with time as the ladle progressively empties. In order to maintain a constant casting throughout, the ladle outlet area is correspondingly enlarged. However, in the present investigation, the constant casting rate has been modeled by assuming a constant melt stream velocity and an invariant tundish inlet area. The temperature of the incoming melt stream

at the beginning of teeming was assumed to be 1838 K (1565°C). It was assumed to drop at a rate of 0.5°C/min over the 50 min of teeming period. Thus, the incoming melt stream temperature at the end of casting was 1813 K (1540°C), a total temperature drop of 25°C. These are realistic values commonly observed in the industry.

4. Numerical Solution Procedure

Finite difference equations were derived for the governing coupled partial differential equations using an implicit finite difference procedure referred to as SIMPLE (Semi-Implicit Method for Pressure Linked Equations).¹³⁾ The flow domain corresponding to the symmetrical quarter of the tundish was divided into a non-uniform grid of 30 (longitudinal) × 10 (transverse) × 14 (vertical). The steady state formulations of the governing equations were first utilized to calculate the steady state flow and thermal fields in the tundish corresponding to the inlet velocity of 1.52 m/sec and an inlet stream temperature of 1813 K. The inlet melt temperature corresponded to the last temperature of the ladle outlet stream of the previous heat in a sequence casting operation. Using the calculated flow and thermal fields as the initial guesses, unsteady state calculations were carried out over the full casting period of 50 min. The flow and temperature fields in the tundish at the end of 50 min were then used as the initial fields to carry out the calculations for a second successive heat of 50 min duration.

5. Results and Discussions

As mentioned previously, the initial situation considered for the modeling of the varying ladle stream temperature was established in the tundish by considering steady state flow of melt coming in at a velocity of 1.52 m/sec and at a temperature of 1813 K. The velocity distributions in the longitudinal, vertical symmetry plane and in the longitudinal, vertical plane close to the wall are shown in Figs. 2(a) and 2(b), respectively. It should be kept in mind that the magnitude of the plotted velocity vectors in Fig. 2 and subsequent velocity plots are proportional to their lengths. The vector shown at the top of Fig. 2 refers to a scale of 0.05 m sec⁻¹. At some places in the tundish, the velocities exceed 0.05 m sec⁻¹; these vectors have been truncated and cross marks (×) are placed on them. Although these high velocity vectors with marks (×) are not clearly visible, they are in the region upstream of the weir. From Fig. 2, it can be seen that the melt, after being entrained in the region bounded by the weir and the dam, flows predominantly along the top free surface towards the tundish outlet. A recirculatory zone can be observed in the downstream side of the dam. The velocities in this region are smaller compared to the velocities in the remainder of the tundish. Figure 2(b) shows that in the plane adjacent to the wall, the melt flow direction is from the bottom towards the free surface in the weir and dam region. Thereafter, the melt flows along the top free surface and down along the end wall to give rise to an extensive

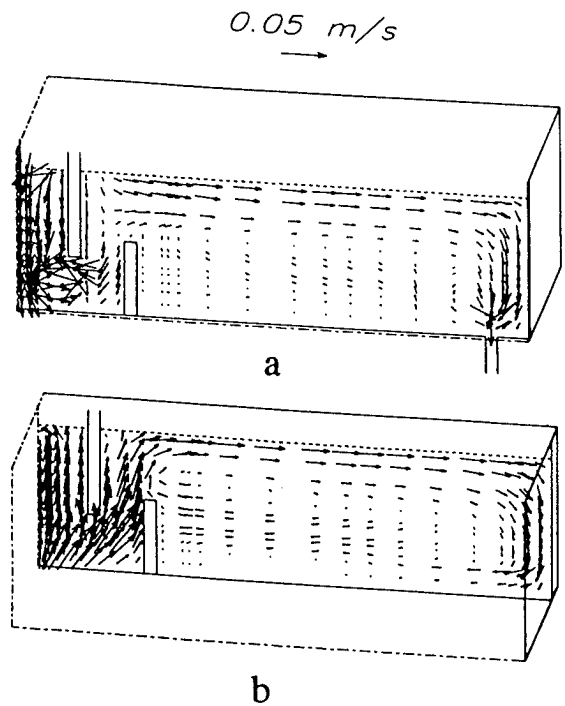


Fig. 2. Predicted flow field in longitudinal, vertical planes, (a) at the plane of symmetry, and (b) closer to the wall under steady state conditions.

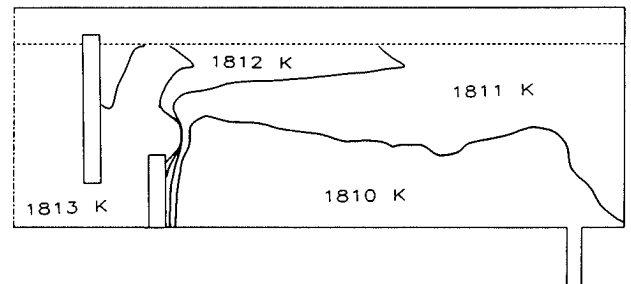


Fig. 3. Temperature distributions in the longitudinal, vertical symmetry plane under steady state conditions.

recirculation in the downstream region of the dam.

Figure 3 represents the temperature contours in the longitudinal, vertical symmetry plane obtained under steady state conditions. From Fig. 3, it can be seen that the high degree of turbulence and consequent mixing has led to the maintenance of the inlet stream temperature of 1813 K in the region bounded by the weir and the dam. As the melt flows along the top surface, it progressively loses heat by radiation. The temperature of the melt drops by about 3°C as it reaches the outlet. The lowest temperatures of 1810 K and below are observed in the relatively stagnant region downstream of the dam.

To trace the evolution of the thermal field of the melt in the tundish corresponding to the varying inlet temperature, four temperature monitoring points within the tundish, A, B, C and D were considered in the mathematical model. The locations of these four monitoring points have been shown in Fig. 1. All of them lie in the longitudinal, vertical symmetry plane of the tundish containing the inlet stream and the exit to the mold. Point A was chosen near the tundish inlet, B near

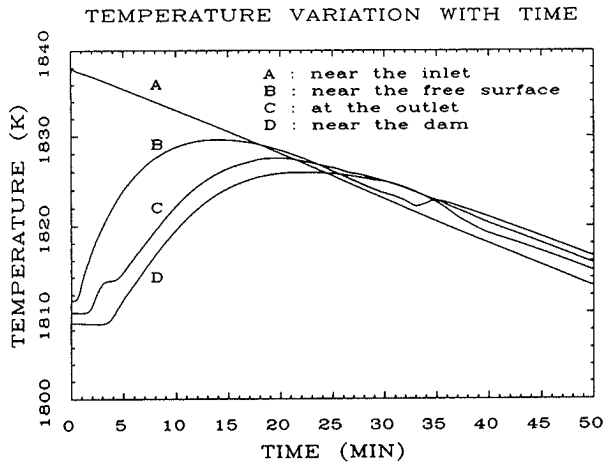


Fig. 4. Temperature variation of the melt at the monitoring points A, near the tundish inlet, B, near the top free surface of the tundish, C, at the tundish outlet and D, near the downstream of the dam, over a full casting period of 50 min.

the free surface, C at the tundish outlet and D near the downstream side of the dam.

Figure 4 represents the temperature variation of the melt at the four monitoring points over the full casting period of 50 min. The temperature at the point A reflects the assumed temperature variation of the melt coming out of the ladle. The incoming stream temperature drops from 1838 to 1813 K over 50 min. However, at the beginning of teeming, the thermal field of the melt in the tundish was assumed to be established by the temperature of the last incoming melt stream of the previous heat, which was 1813 K. The influx of the hotter melt stream of the present heat thus leads to a gradual increase of the overall temperature of the melt within the tundish. This is reflected in the rise of the temperature of the melt at the monitoring points B, C and D. The temperature of the melt near the free surface (B) has increased from about 1812 to about 1828 K during the first 10 min of teeming. The temperatures of the melt at the outlet (C) and near the dam (D) have also increased but at slower rates. The temperature of the melt at the outlet (C) has increased from 1810 to about 1822 K during the same time, whereas the temperature at the region downstream of the dam and adjacent to it (D) has increased from about 1809 to about 1820 K.

The effect of the continuous decrease of the incoming melt temperature on the temperature of the melt in the tundish beyond the initial 10 min of teeming can also be seen from Fig. 4. The temperature of the melt at B near the free surface attains a maximum of about 1829 K, after 15 min of pouring and then starts to fall. The tundish outlet melt temperature (C), however, continues to increase for about 5 more min and reaches its highest value of about 1827 K before starting a very gradual decline. The temperature of the melt just downstream of the dam (D) also reaches its maximum at about 1826 K after 20 min of teeming.

The changes in the temperature field in the melt in the longitudinal, vertical plane containing the inlet stream and the exit to the mold, over the first 20 min of teeming

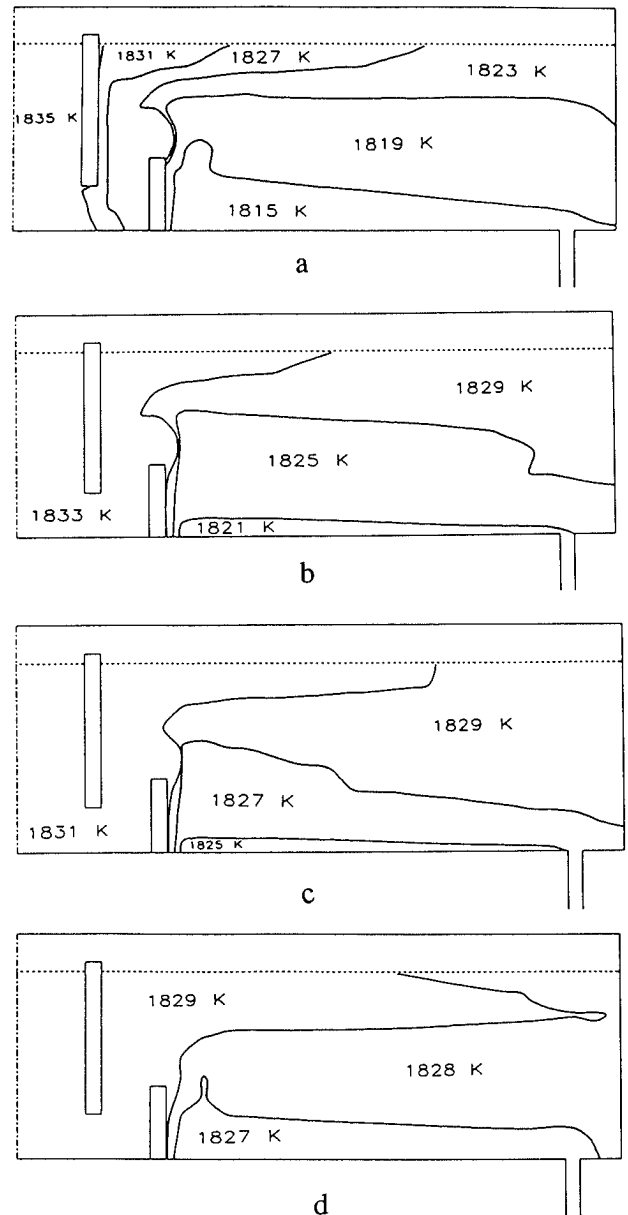


Fig. 5. Temperature distributions in the longitudinal, vertical symmetry plane, a) 5 min, b) 10 min, c) 15 min and d) 20 min from the start of teeming.

is depicted in Fig. 5. Figure 5(a) represents the temperature contours after 5 min of teeming, while Figs. 5(b), 5(c) and 5(d) represent the same after 10, 15 and 20 min of teeming, respectively. It can be seen from Fig. 5(a) that there is significant temperature stratification of the melt in the tundish during the initial stages of teeming. The highest temperature region of 1835 K exists upstream of the weir while the melt flowing out to the mold is at a temperature of 1815 K. Thus, there is a temperature gradient of about 20°C between the inlet and the outlet with progressively lower temperatures from the top free surface of the melt to the bottom of the tundish. As teeming progresses, the degree of temperature stratification decreases (Figs. 5(b), 5(c)) until the temperature differential in the melt between the inlet and the outlet has decreased to about 2°C after 20 min of teeming (Fig. 5(d)).

Figure 6 represents the predicted velocity profiles in

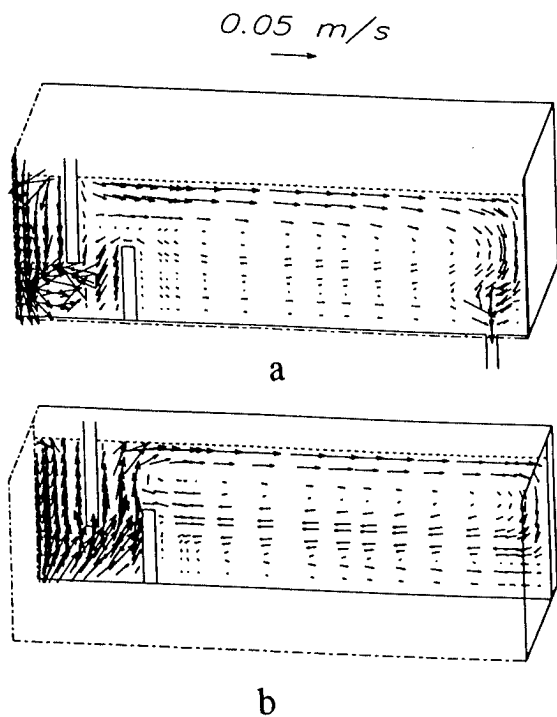


Fig. 6. Predicted flow field in longitudinal, vertical planes, (a) at the plane of symmetry, and (b) closer to the wall after 10 min of teeming.

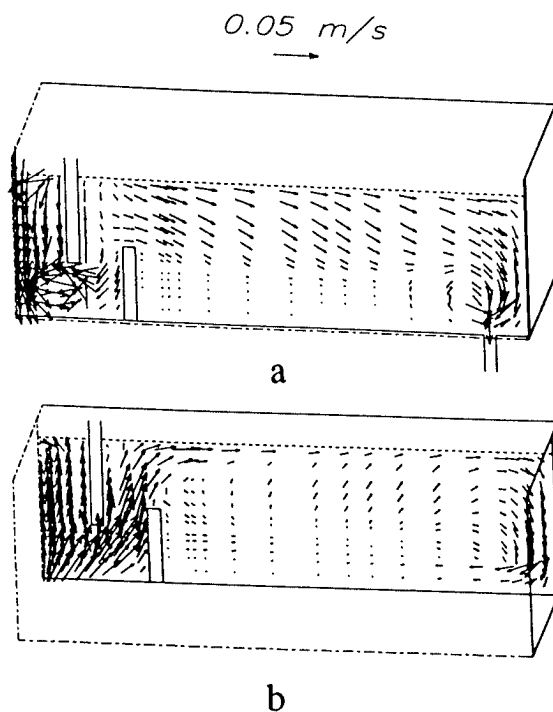


Fig. 7. Predicted flow field in longitudinal, vertical planes, (a) at the plane of symmetry, and (b) closer to the wall after 25 min of teeming.

the tundish after a teeming period of 10 min. Figure 6(a) represents the velocity field in the longitudinal, vertical symmetry plane while Fig. 6(b) shows the velocity field near the wall. It can be seen that the significant temperature stratification existing in the tundish (Fig. 5(b)) has not resulted in any significant deviations from the corresponding steady state velocity fields (compare Figs. 2 and 6), except for a slightly stronger recirculation of the melt from the outlet region towards the dam (Fig. 6(b)). Figure 6 is also representative of the velocity fields existing in corresponding planes of the tundish after 5, 15 and 20 min of teeming. Thus, it can be seen that the actual extent of temperature stratification of the melt between the inlet and the outlet (20°C after 5 min of teeming or 2°C after 20 min of teeming) does not have any significant effect on the flow profile of the melt within the tundish. The density of melt decreases as the temperature of the melt is increased. Thus, due to buoyancy effects, a lighter, higher temperature melt will always tend to flow up and above a heavier, cooler melt. The presence of the dam also helps in directing the flow of the melt towards the free surface. The overall top free surface directed flow seen hitherto in the tundish is guaranteed as long as the temperature of the melt coming in through the inlet is higher than the bulk temperature of the melt in the tundish.

Figure 7 represents the predicted velocity fields in the same longitudinal, vertical planes of the tundish after a teeming period of 25 min. The flow patterns are seen to be dramatically different from those seen hitherto. By this time, the temperature of the incoming melt has dropped to such an extent where the melt coming out of the weir-dam region is cooler than the melt in the remainder of the tundish. Due to the buoyancy effects,

the denser, cooler melt tends to move downwards instead of flowing along the top free surface, which is more apparent at the symmetry plane (Fig. 7(a)). Near the wall, (Fig. 7(b)), the appreciable velocities of the melt along the top free surface, seen in the first 20 min or so, are absent. It can be seen from Fig. 4 that the temperature differential between the cooler incoming melt and the existing hotter melt in the tundish is of the order of $1\text{--}2^{\circ}\text{C}$. However, it is sufficient to initiate a complete reversal of the flow pattern of the melt which is maintained over the rest of the teeming period.

Figures 8(a), 8(b), 8(c) and 8(d) represent the predicted velocity fields in the longitudinal, vertical symmetry plane of the tundish containing the inlet stream and the exit to the mold, after a teeming period of 35, 40, 45 and 50 min respectively. They show the gradual development of the inverse recirculatory flow pattern occurring due to the temperature inversion. Cooler fluid coming through the inlet meets the hotter fluid downstream of the dam, sinks along the dam and flows towards the outlet region. The melt flow is thus predominantly along the bottom, a situation exactly opposite to the predominantly top free surface directed flow observed in the tundish for the first 20 min of teeming. A backward recirculatory flow pattern develops near the top free surface (Fig. 8(a)) from the region near the outlet towards the weir. This basic flow pattern gradually develops (Figs. 8(b) and 8(c)) and envelops the bulk of the tundish downstream of the dam as teeming progresses until 50 min (Fig. 8(d)). The flow patterns, at various times, in all the other longitudinal, vertical planes of the tundish are similar to the corresponding flow fields existing at the symmetry plane; hence they are not represented here.

The inverse flow pattern existing in the tundish from

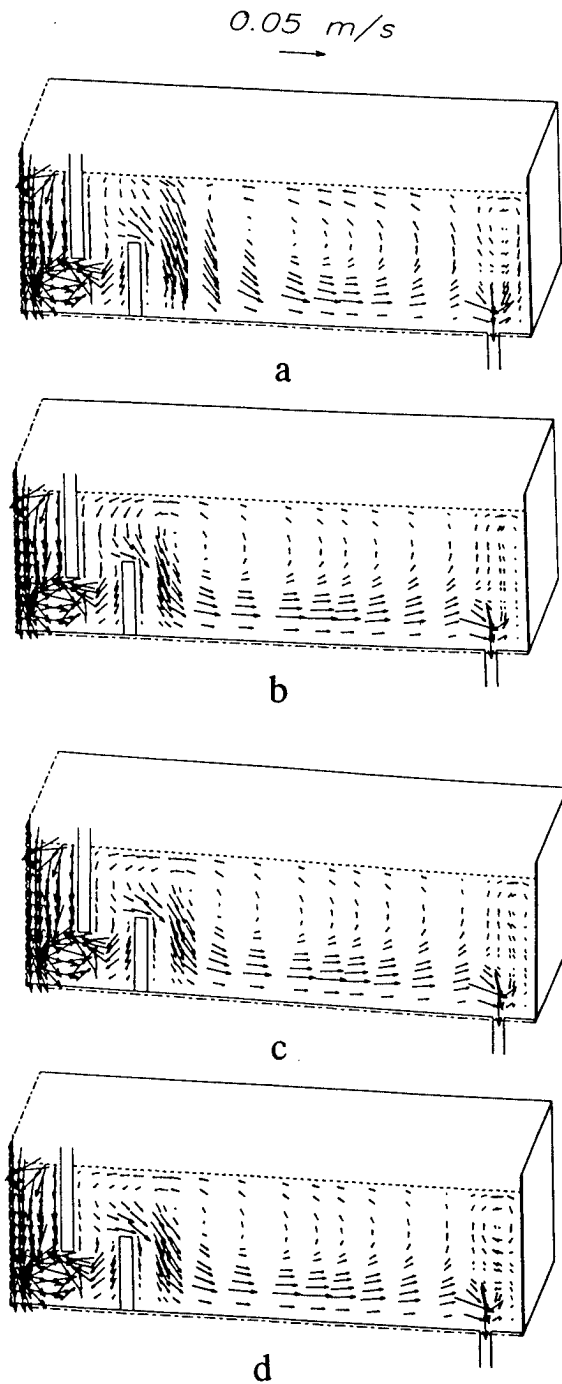


Fig. 8. Predicted flow field in the longitudinal, vertical symmetry plane after (a) 35 min, (b) 40 min, (c) 45 min and (d) 50 min of teeming.

about 25 min of pouring of the melt until the end of the teeming period has important consequences as far as inclusion flotation and removal are concerned. It can be seen that prior to the initiation of the downward directed flow pattern, the dam and the weir have been effective in directing the bulk of the melt up and along the top surface. This free surface directed flow is essential for efficient inclusion flotation and removal since it directs the inclusions towards the free surface aiding in floatout and also increases the contact time of the melt with the top slag layer as it flows adjacent to it. However, this beneficial effect of the flow control devices is seen to be completely negated by the temperature inversion phe-

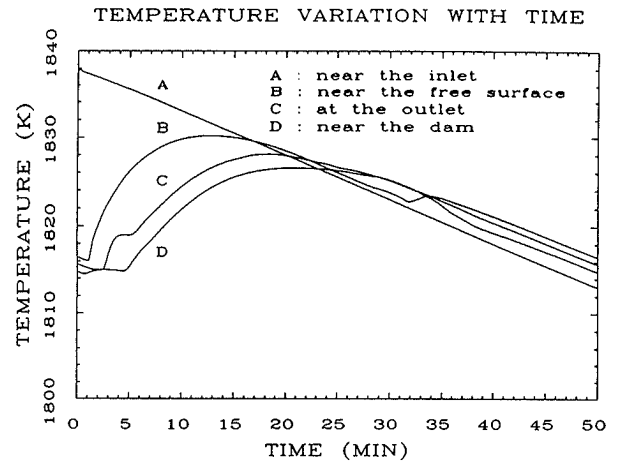


Fig. 9. Temperature variation of the melt at the monitoring points A, near the tundish inlet, B, near the top free surface of the tundish, C, at the tundish outlet and D, near the downstream of the dam, over a successive casting period of 50 min.

nomenon. Now, the bulk of the fluid flows along the bottom of the tundish on its way to the outlet. Thus, under the conditions assumed in these calculations, the overall flow pattern is expected to be along the bottom of the tundish for the last 25 min of teeming, leading to very poor rate of inclusion flotation and removal. An appreciable melt velocity along the bottom may also lead to refractory wear which in turn will lead to an increase in the number of exogenous inclusions. Thus, the products cast during the beginning of a new ladle⁴⁾ and the end of a teeming period (due to temperature inversion) are expected to have higher inclusion contents compared to the products cast during the rest of the teeming period.

It has to be appreciated that the initial conditions utilised for the transient calculations of the temperature and flow fields in the tundish for the 50 min teeming period were obtained from the steady state calculations with an inlet temperature of 1813 K. The steady state melt temperature at the outlet was 1810 K. However, from the above discussion it can be seen that the melt temperature at the outlet is expected to be about 2°C higher than the melt temperature near the tundish inlet at the end of a heat. For proper simulation of an intermediate heat in a sequence casting operation, the initial field should be that at the end of teeming of the previous heat. Accordingly, the mathematical modeling of the next heat was carried out with the initial conditions being those existing in the tundish after 50 min of teeming of the recently completed heat.

Figure 9 represents the temperature histories of the melt at the same four monitoring points within the tundish for the following heat. It can be seen from comparison of Figs. 4 and 9 that, except for some expected differences in temperature values of the melt during the corresponding initial stages of teeming, the overall pattern of the time-temperature histories are similar. The temperature of the melt near the free surface (B) increases to about 1830 K after 10 min of teeming. The temperature of the melt near the outlet continues to

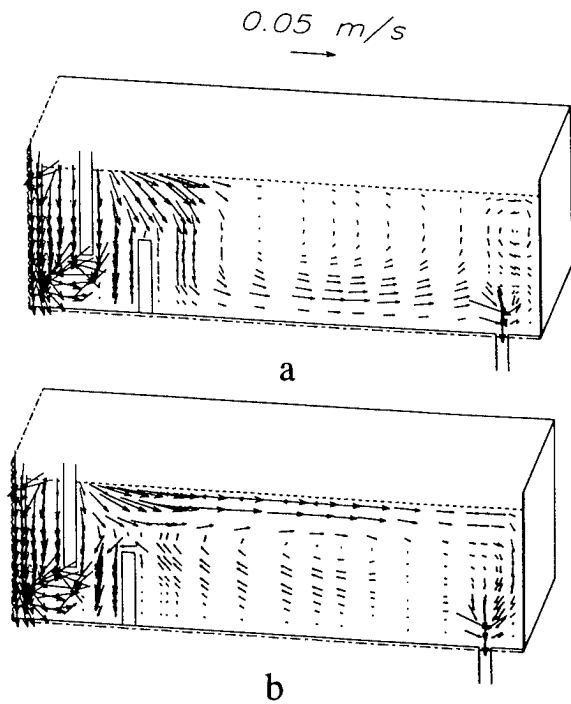


Fig. 10. Predicted flow field in the longitudinal, vertical symmetry plane after (a) 1 min, and (b) 2 min of teeming of the second successive heat.

decline for the first three minutes of teeming, reflecting the time taken by the effect of the first hot metal of the new heat to reach the tundish outlet. Thereafter, the temperature of the melt exiting the tundish rises to about 1828 K after about 20 min of teeming. The temperature of the melt at the point D near the dam also peaks to about 1826 K after 20 min of teeming.

Figures 10(a) and 10(b) represent the velocity fields in the longitudinal, vertical symmetry plane of the tundish, after 1 and 2 min of teeming of the new heat respectively. It can be seen that the inverse flow pattern persists for about 1 min into the casting of the new heat while the flow pattern reverts to the top free surface directed flow within the next minute. The subsequent velocity profiles at various times of teeming of the second heat are identical to those calculated corresponding to the previous heat and are not repeated here. The melt flow direction reverts to the bottom directed flow after about 25 min of teeming, corresponding to the inlet melt temperature being 1–2°C cooler than the bulk melt temperature. The flow reversal phenomena persists until the end of the second heat.

The flow reversal phenomena corresponding to a 1–2°C difference in the steel temperatures between the outlet and the inlet of the tundish has been corroborated by appropriately scaled water modeling studies carried out at The Ohio State University. Injection of colored water into the inlet stream has helped in the demonstration of the flow reversal effect when cooler fluid is poured into the model tundish containing water at a uniform temperature.

It has to be kept in mind that the temperature inversion phenomena and the attendant flow reversal effect are not expected to occur every time molten metal is teemed from

a ladle to a tundish. The flow reversal phenomena is due to the coupling of heat transfer and fluid flow characteristics of the melt in the tundish and hence should be dependent on the thermal state of the melt in the ladle, the heat transfer characteristics of the ladle and the tundish, casting rate and other relevant operating parameters. The above mathematical modeling has been done under the assumption of identical thermal cycles of the ladle during successive heats. In actual operation, the superheats of the melt contained in the ladle may vary from heat to heat. If, for example, the second heat was considered to start pouring at a temperature higher than the 1838 K assumed in the present study, the inlet melt temperature might remain higher than the melt temperature in the bulk of the tundish for most of the casting period. Conversely, if the superheat of the melt to be cast in the subsequent heat was lower than 1838 K, the temperature inversion phenomena might initiate earlier than 25 min from the beginning of teeming. The heat loss rates through the various ladle surfaces will also determine whether the temperature inversion phenomena will occur during a heat. Improvement of the ladle refractory linings, utilisation of a thicker slag cover along with the use of a refractory ladle cover will lead to lower rates of heat loss. An actual temperature drop rate of the ladle melt stream, lower than the 0.5°C/min value considered in the present modeling study, may be sufficient to avert the flow reversal phenomena and the consequent deleterious effect on inclusion flotation and removal in the tundish. Conversely, the rate of heat loss from the ladle can increase over successive heats. This is due to the gradual wear of the refractory linings of the ladle through successive heats leading to increased rates of conductive heat losses. Thus, the flow reversal phenomena may appear in the tundish during the later heats teemed from the same ladle.

The heat transfer characteristics of the tundish can also determine whether or not temperature inversion phenomena will occur in the tundish during teeming. With reference to Fig. 4 or Fig. 9, it can be seen that if the heat loss rates through the various tundish surfaces are increased, the temperatures of the melt in the tundish at the various points might peak and decay in such a way that the temperatures of the melt in the bulk of the tundish is always lower than that of the melt coming in through the inlet. It suffices to maintain the temperature of the incoming melt stream 1–2°C higher than the bulk temperature of the melt in the tundish, to maintain the free surface directed flow for the entire casting period. All other factors remaining the same, a similar effect can be expected for a lower casting rate of the melt. The melt will now spend longer time within the tundish thus enabling more heat to be extracted through the various tundish surfaces.

Thus, a complex interplay of factors determines whether or not the temperature inversion with the attendant flow reversal phenomena is expected in a tundish during a certain heat. The present mathematical model can be utilized to examine the various conditions under which the above phenomena can be avoided. Thus,

it can serve as a valuable process optimization tool in the drive towards casting of superior quality steels.

6. Summary and Conclusions

A mathematical model to represent melt flow and heat transfer in a typical continuous slab casting tundish under varying inlet stream temperature condition has been developed. The incoming melt stream temperature has been assumed to decline at a constant rate of $0.5^{\circ}\text{C}/\text{min}$ of a typical 50 min casting period. After about 25 min of teeming, the incoming melt becomes cooler than the melt in the bulk of the tundish by about $1\text{--}2^{\circ}\text{C}$ and starts to flow along the bottom instead of the top free surface. This inverse flow pattern develops and continues over the remaining 25 min of the teeming period but reverts to the normal free surface directed flow within the first 2 min of teeming of the next heat in a sequence casting operation. The inverse flow pattern reappears after about 25 min of teeming of the new heat. Under the conditions examined in this paper, the steel cast during the last 25 min of the heat is expected to have a higher inclusion content than the one cast during the rest of the teeming period. The present mathematical modeling study has shown that the fluid flow and heat transfer characteristics of the melt in the tundish cannot be treated in isolation, but have to be coupled with the heat transfer characteristics of the ladle for realistic simulation of the continuous casting process.

Acknowledgements

This work has been supported by The National Science Foundation, Grant No. MSM-8602523 and The National Steel Technical Research Center.

Nomenclature

- C_1, C_2, C_D : Constants in the $k\text{--}\epsilon$ turbulence model
 G : Generation of turbulence energy, defined by Eq. (5)
 g_i : Acceleration due to gravity in the i^{th} direction

- (m sec^{-2})
 k : Turbulent kinetic energy ($\text{m}^2 \text{sec}^{-1}$)
 k_{eff} : Effective thermal conductivity ($\text{W m}^{-1} \text{K}^{-1}$)
 p : Pressure ($\text{kg m}^{-1} \text{sec}^{-2}$)
 T : Temperature (K)
 t : Time (sec)
 u_i, u_j : Mean velocity in the $i^{\text{th}}, j^{\text{th}}$ direction (m sec^{-1}), $i, j=1, 2, 3$ denoting the three cartesian coordinate directions
 ϵ : Dissipation rate of turbulent kinetic energy ($\text{m}^2 \text{sec}^{-3}$)
 μ_l : Molecular viscosity ($\text{kg m}^{-1} \text{sec}^{-1}$)
 μ_t : Turbulent viscosity ($\text{kg m}^{-1} \text{sec}^{-1}$)
 μ_{eff} : Effective viscosity ($\text{kg m}^{-1} \text{sec}^{-1}$)
 ρ : Density of the fluid (kg m^{-3})
 ρ_0 : Reference density of the fluid (kg m^{-3})
 $\sigma_k, \sigma_\epsilon$: Schmidt number for k and ϵ

REFERENCES

- 1) Y. He and Y. Sahai: *Metall. Trans. B*, **18B** (1987), 81.
- 2) J. Szekely and O. Ilegbusi: *The Physical and Mathematical Modeling of Tundish Operations*, Springer-Verlag, New York, (1989).
- 3) S. Joo, R. Guthrie and C. Dobson: *Steelmaking Proceedings*, Vol. 72, ISS-AIME, Chicago, (1989), 401.
- 4) S. Chakraborty and Y. Sahai: *Proc. Sixth Int. Iron & Steel Cong.*, Vol. 3, ISIJ, Tokyo, (1990), 189.
- 5) R. A. Weber: *Ironmaking Steelmaking*, **8** (1981), No. 5, 201.
- 6) R. Baker and W. R. Irving: *Ironmaking Steelmaking*, **8** (1981), No. 5, 216.
- 7) R. L. Minion and C. F. Leckie: *Steelmaking Proceedings*, Vol. 69, ISS-AIME, Washington, (1986), 335.
- 8) B. Launder and D. Spalding: *Heat Transfer Section Report No. HTS/73/2*, Imperial College, London, (1973).
- 9) B. Launder and D. Spalding: *Computer Methods in Applied Mechanics and Engineering*, Vol. 3, (1974), 269.
- 10) Private communication with Dr. K. Kaul, Natco Inc., (1990).
- 11) C. Jayatilke: *Progress in Heat and Mass Transfer*, Vol. 1, (1969), 193.
- 12) J. Holman: *Heat Transfer*, Mc-Graw Hill, New York, (1981).
- 13) S. V. Patankar: *Numerical Heat Transfer and Fluid Flow*, Hemisphere Publishing Corp., (1980).